Energy Materials

Supplementary Material

Theoretical evidence of self-intercalated 2D materials for battery and electrocatalytic applications

Theoretical evidence of self-intercalated 2D materials for battery and electrocatalytic applications

Ke Fan[1,2], Yuen Hong Tsang[1,3,*], Haitao Huang[1,2,*]

[1]Department of Applied Physics, The Hong Kong Polytechnic University, Hung Hom, Kowloon, Hong Kong 999077 China.
[2]Research Institute for Smart Energy, The Hong Kong Polytechnic University, Hung Hom, Kowloon, Hong Kong 999077 China.
[3]Photonic Research Institute, The Hong Kong Polytechnic University, Hung Hom, Kowloon, Hong Kong 999077 China.

***Correspondence to:** Dr. Yuen Hong Tsang, Department of Applied Physics, The Hong Kong Polytechnic University, 11 Yuk Choi Rd, Hung Hom, Kowloon, Hong Kong 999077 China. E-mail: yuen.tsang@polyu.edu.hk. Prof. Haitao Huang, Department of Applied Physics, The Hong Kong Polytechnic University, 11 Yuk Choi Rd, Hung Hom, Kowloon, Hong Kong 999077 China. E-mail: aphhuang@polyu.edu.hk

MAIN TEXT

Additional computational details

The differential charge density of lithium adsorption as a function of space was obtained as the difference between the valence charge density before and after the bonding:

$$\Delta\rho(\vec{r}) = \rho_{M_7S_{12}\mathrm{Li}}(\vec{r}) - \rho_{M_7S_{12}}(\vec{r}) - \rho_{Li}(\vec{r}) \quad \text{(S1)}$$

where $\rho_{M_7S_{12}\mathrm{Li}}(\vec{r})$, $\rho_{M_7S_{12}}(\vec{r})$, and $\rho_{Li}(\vec{r})$ represent the charge density distributions of Li adsorbed on M_7S_{12} systems, bare M_7S_{12} monolayer, and Li atom, respectively.

Supplementary Table 1. DFT-optimized lattice constants *a*, *b*, heights *h*, and bond lengths d_1, d_2, and d_3 of seven stable ic-2D crystals.

System	*a* (Å)	*b* (Å)	*h* (Å)	d_1 (Å)	d_2 (Å)	d_3 (Å)
Ti_7S_{12}	5.92	5.92	8.68	2.40	2.48	2.46
V_7S_{12}	5.64	5.67	8.42	2.40	2.30	2.29
Cr_7S_{12}	5.79	5.77	8.28	2.34	2.39	2.39
Mn_7S_{12}	5.76	5.77	8.37	2.32	2.38	2.42
Fe_7S_{12}	5.56	5.56	7.46	2.40	2.26	2.33
Co_7S_{12}	5.77	5.77	7.20	2.25	2.28	2.29
Ni_7S_{12}	5.83	5.83	7.58	2.27	2.28	2.37

Supplementary Table 2. DFT-calculated cohesive energies E_{coh} in eV/atom of 7 ic-2D crystals.

	Ti_7S_{12}	V_7S_{12}	Cr_7S_{12}	Mn_7S_{12}	Fe_7S_{12}	Co_7S_{12}	Ni_7S_{12}
E_{coh} (eV)	-6.44	-5.86	-6.45	-4.52	-4.70	-4.87	-4.08

Supplementary Table 3. In-plane elastic constants, Young's modulus Y and Poisson's ratio ν of 7 ic-2Ds.

	C_{11}[a] (N/m)	C_{12}[a] (N/m)	C_{66} (N/m)	Y (N/m)	ν
Ti_7S_{12}	58.45	7.50	24.54	28.97	0.18
V_7S_{12}	56.55	10.03	23.19	27.17	0.19
Cr_7S_{12}	40.70	4.02	18.78	21.15	0.14
Mn_7S_{12}	4.92	-6.75	6.665	11.51	0.58
Fe_7S_{12}	62.64	9.96	27.61	32.05	0.18

Co_7S_{12}	46.15	14.63	16.49	20.77	0.24
Ni_7S_{12}	53.25	16.03	18.64	24.65	0.26

[a]$C_{22}=C_{11}$; $C_{21}=C_{12}$. Young's moduli $Y=Yx=Yy=(C_{11}C_{22}-C_{12}C_{21})/C_{11}$; Poisson's ratio $\nu = C_{12}/C_{11}$

Supplementary Table 4. Total energy of Li atom adsorbed on 2×2×1 supercell of ic-2Ds (eV) at various adsorption sites from the same side of the materials. Some initial structures transform to a more stable geometry after DFT relaxation.

	Site 1	**Site 2**	**Site 3**	**Site 4**	**Site 5**	**Site 6**
$Ti_7S_{12}Li$	-538.29	-538.28	-538.26	-537.32	-538.46	-537.32
$V_7S_{12}Li$	-536.52	-536.34	-536.30	-536.63	-536.83	-536.83
$Cr_7S_{12}Li$	-529.99	-529.61	-529.72	-529.91	-529.76	-529.85
$Mn_7S_{12}Li$	-510.14	-509.94	-509.12	-509.65	-510.77	-510.10
$Fe_7S_{12}Li$	-476.47	-476.47	-475.51	-474.64	-475.40	-473.72
$Co_7S_{12}Li$	-439.08	-438.96	-438.96	-438.16	-438.97	-438.99
$Ni_7S_{12}Li$	-386.43	-386.28	-386.28	-386.72	-386.73	-385.81

Supplementary Table 5. Adsorption energy of hydrogen atom (eV) at various adsorption sites of ic-2Ds from the same side of the materials. Certain initial sites transform to a more stable geometry after relaxation.

	Site 1	**Site 2**	**Site 3**
$Ti_7S_{12}H$	-2.81	-2.81	**-3.06**
$V_7S_{12}H$	-3.74	-3.31	**-3.75**
$Cr_7S_{12}H$	**-3.79**	-3.48	-1.79
$Mn_7S_{12}H$	-1.47	-1.46	**-2.46**
$Fe_7S_{12}H$	-4.05	**-4.15**	-4.05
$Co_7S_{12}H$	**-4.00**	-3.06	-4.00
$Ni_7S_{12}H$	**-3.63**	-3.63	-3.63

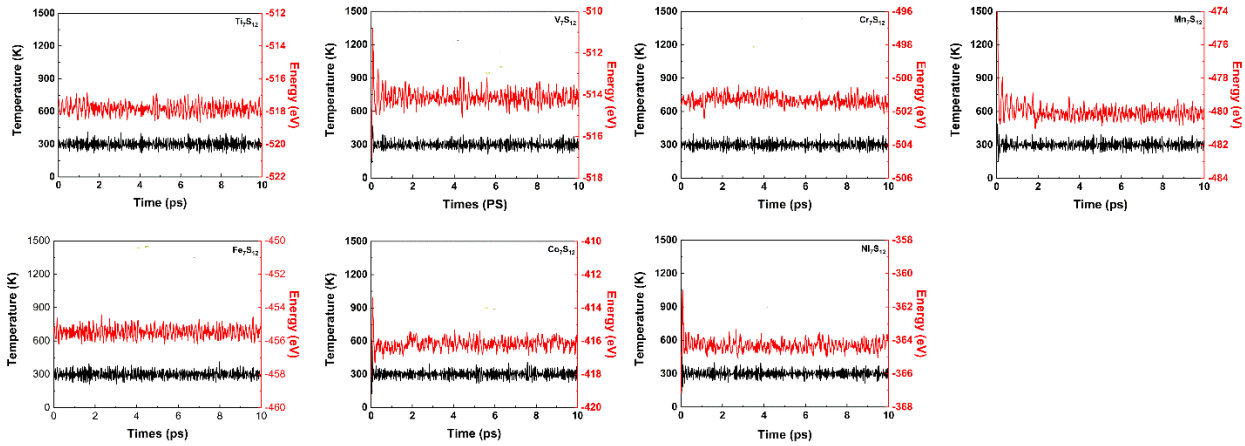

Supplementary Figure 1. Total energy and temperature as a function of time during the AIMD simulations at 300 K for ic-2D crystals.

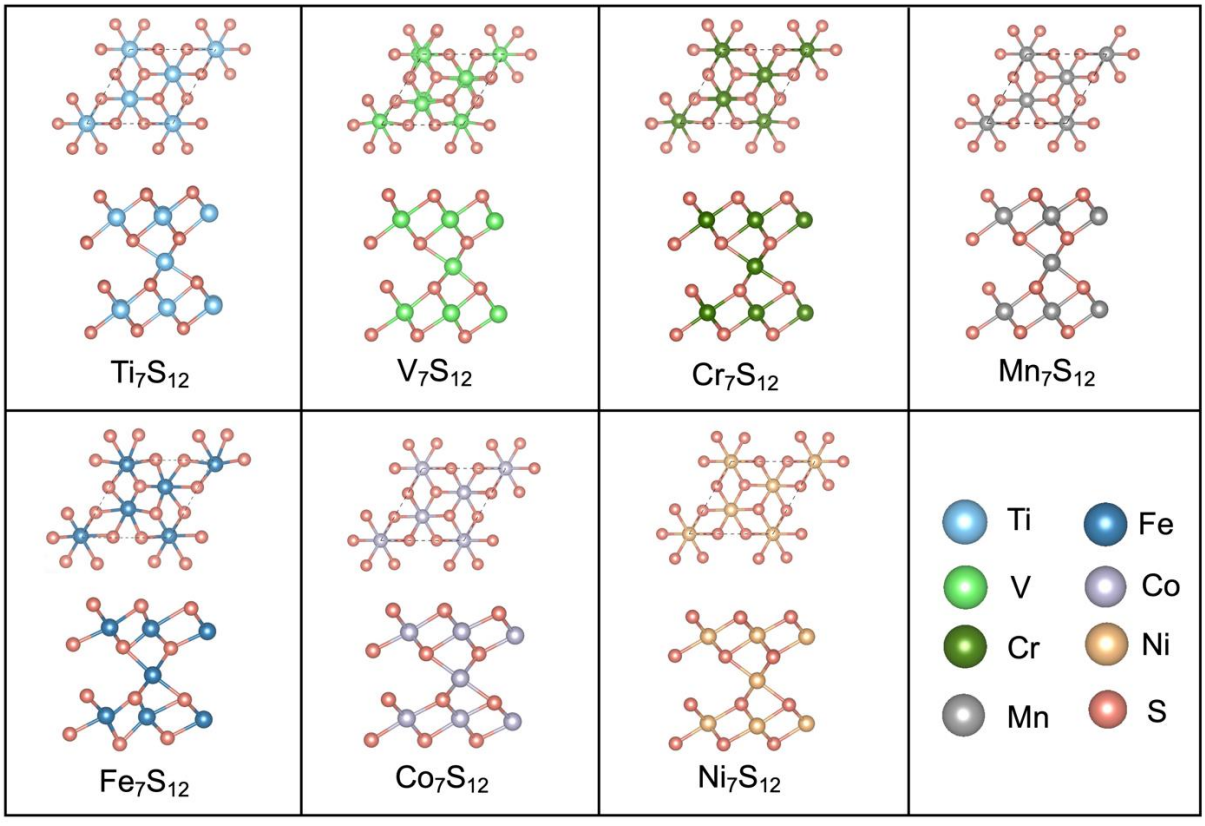

Supplementary Figure 2. Optimized structures of seven representative stable ic-2D crystals: (a) Ti_7S_{12}, (b) V_7S_{12}, (c) Cr_7S_{12}, (d) Mn_7S_{12}, (e) Fe_7S_{12}, (f) Co_7S_{12}, and (g) Ni_7S_{12}.

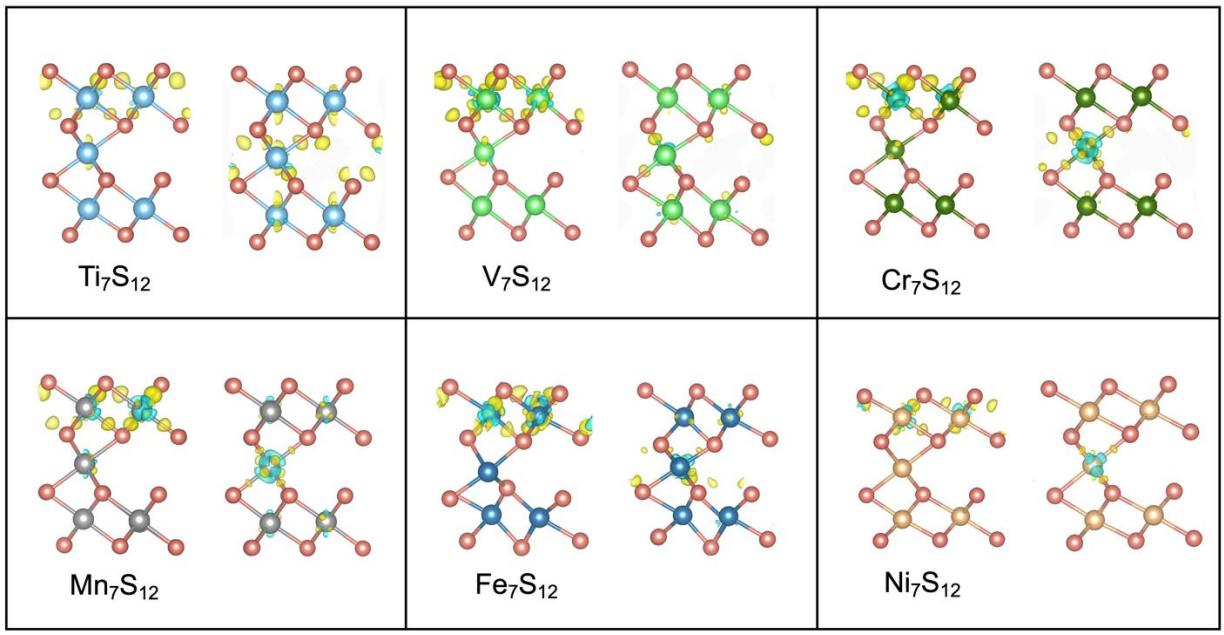

Supplementary Figure 3. Differential charge density distributions of Ti_7S_{12}, V_7S_{12}, Cr_7S_{12}, Mn_7S_{12}, Fe_7S_{12}, and Ni_7S_{12}.

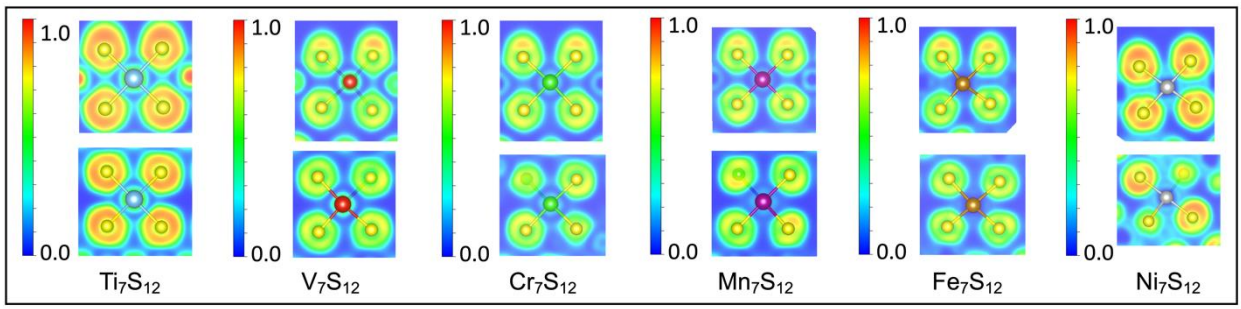

Supplementary Figure 4. Electron localization function (ELF) maps of Ti_7S_{12}, V_7S_{12}, Cr_7S_{12}, Mn_7S_{12}, Fe_7S_{12}, and Ni_7S_{12}.

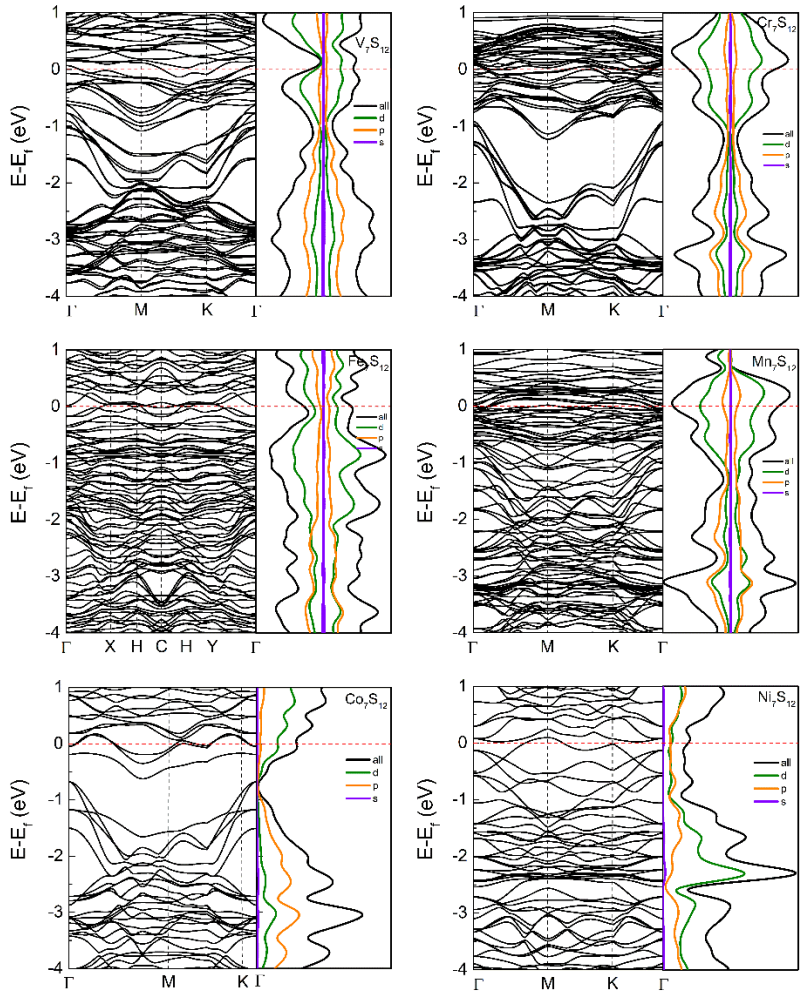

Supplementary Figure 5. Electronic band structures (left panel) and total and projected density-of-states (DOS) plots (right panel) of ic-2Ds. Fermi level is set at 0 eV.

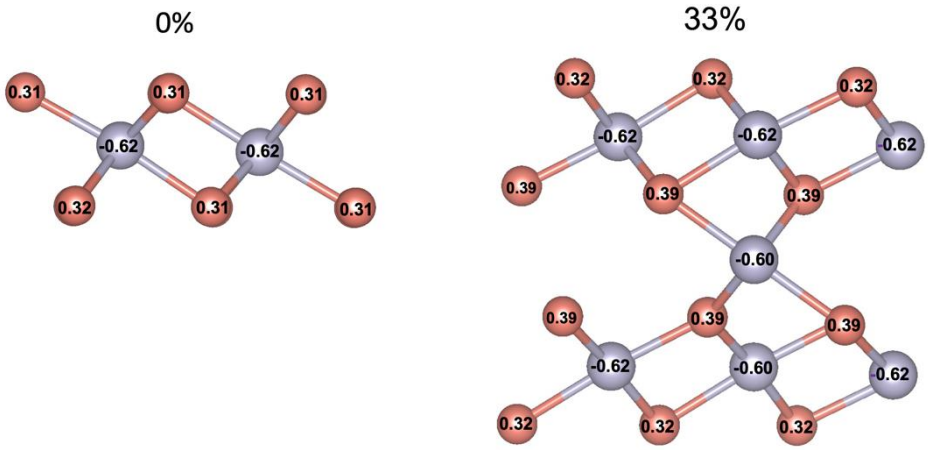

Supplementary Figure 6. Variation of the Bader charge in Co and S atoms in CoS_2 and Co_7S_{12}.

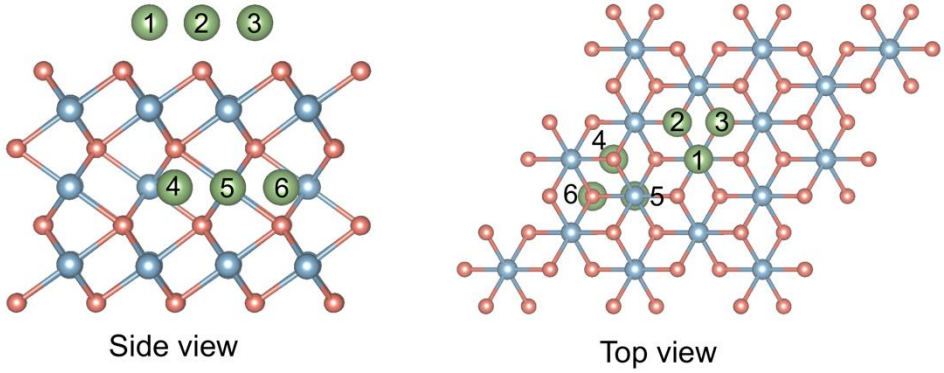

Supplementary Figure 7. Six possible high-symmetry adsorption sites on the surface of ic-2D crystals.

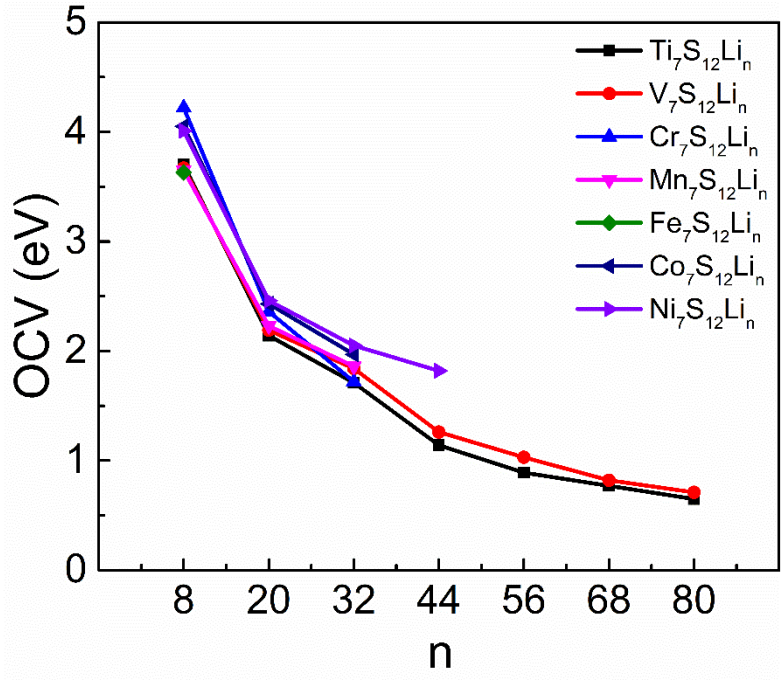

Supplementary Figure 8. OCV as a function of the number of adsorbed Li atoms for ic-2D crystals.

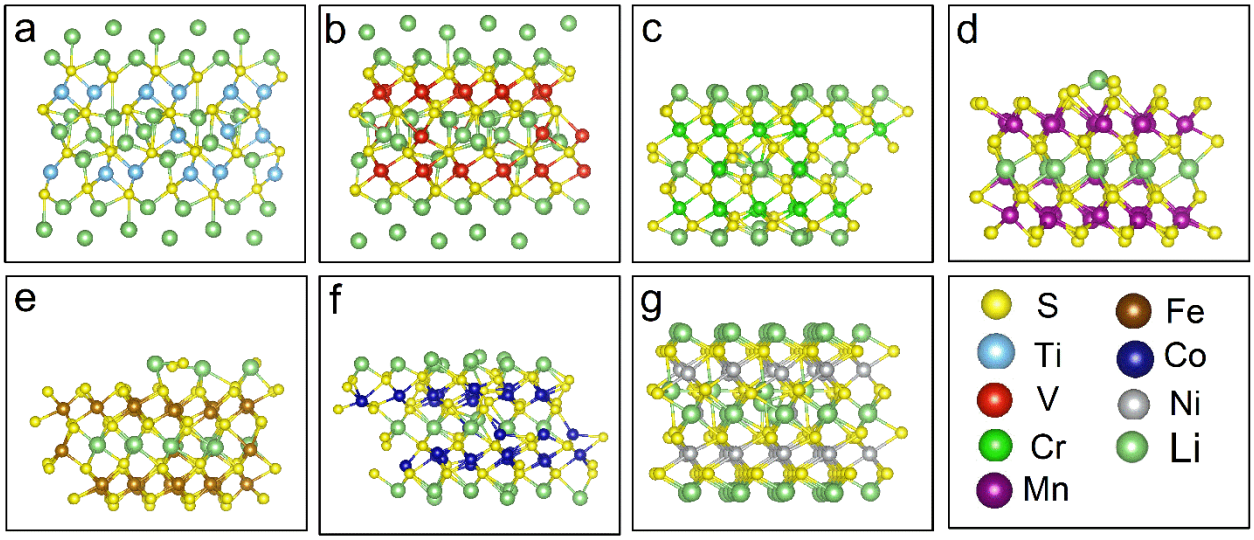

Supplementary Figure 9. Optimized structures of different Li-intercalated ic-2Ds (2×2 supercell) with the maximum lithium intercalation content. (a) Ti_7S_{12}, (b) V_7S_{12}, (c) Cr_7S_{12}, (d) Mn_7S_{12}, (e) Fe_7S_{12}, (f) Co_7S_{12}, and (g) Ni_7S_{12}.

Here, we consider the adsorption of lithium on the single side and determined that lithium adsorbs unilaterally on the substrate up to a maximum of two layers above ic-2D (Layer 2 and Layer 4 in **Figure 4A**). If it continues to adsorb onto the third layer on the single side, due to the larger distance between the adsorbed ions, there is no significant chemical interaction between them. As a result, the theoretical capacities of the ic-2D materials were calculated based on seven lithium layers, including four layers above and below the ic-2D (two layers per side) and three interlayers (Layer 1, Layer 3 in Figure 4A, and the equivalent layer of Layer 3 below Layer 1). The optimized structures of different Li-intercalated ic-2Ds (2×2 supercell) with the maximum lithium intercalation content are shown in Supplementary Figure 9, where the seven-layer adsorption pattern can be observed for Ti_7S_{12} and V_7S_{12}.

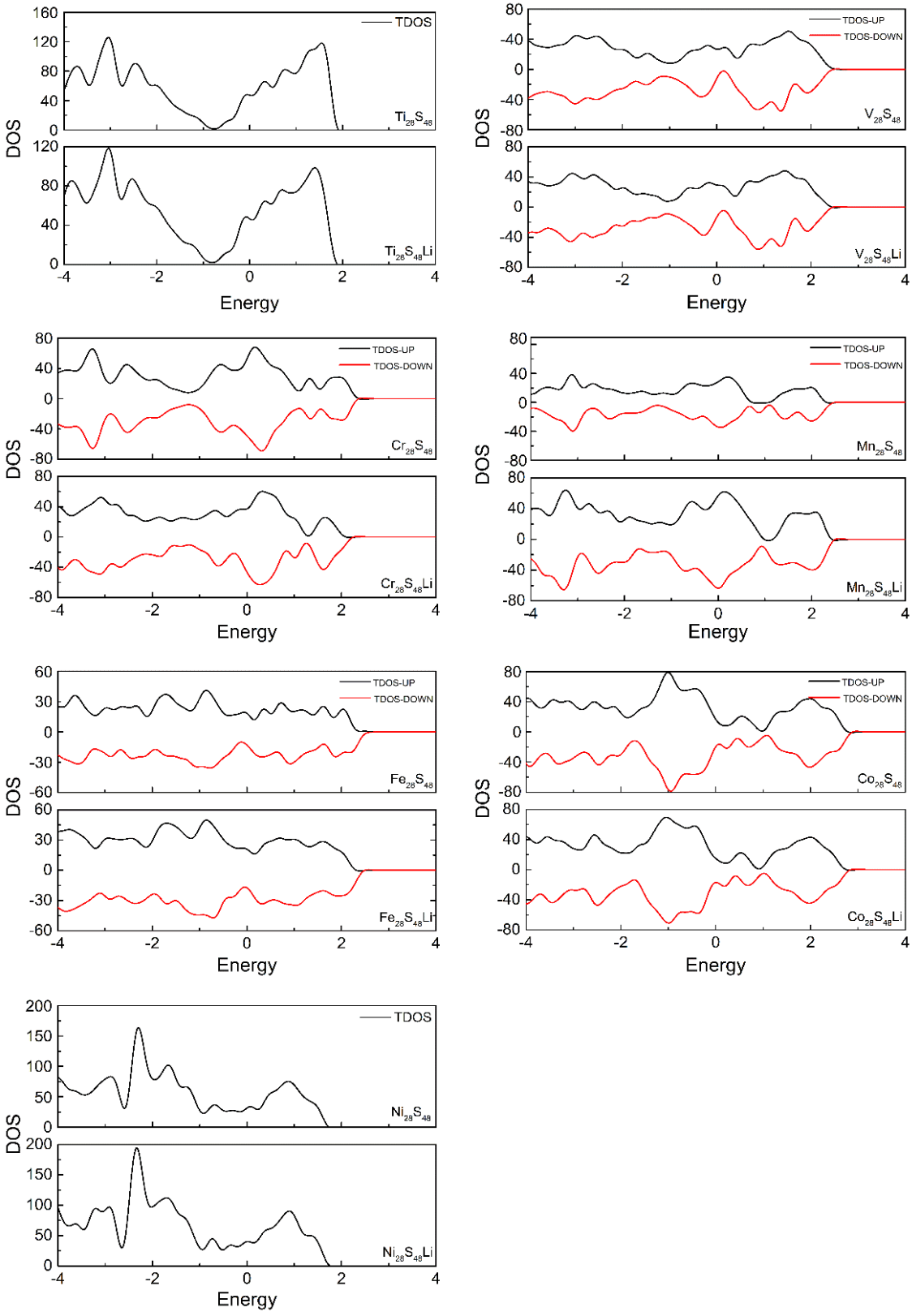

Supplementary Figure 10. Density of states of pure ic-2Ds and Li-intercalated ic-2Ds.

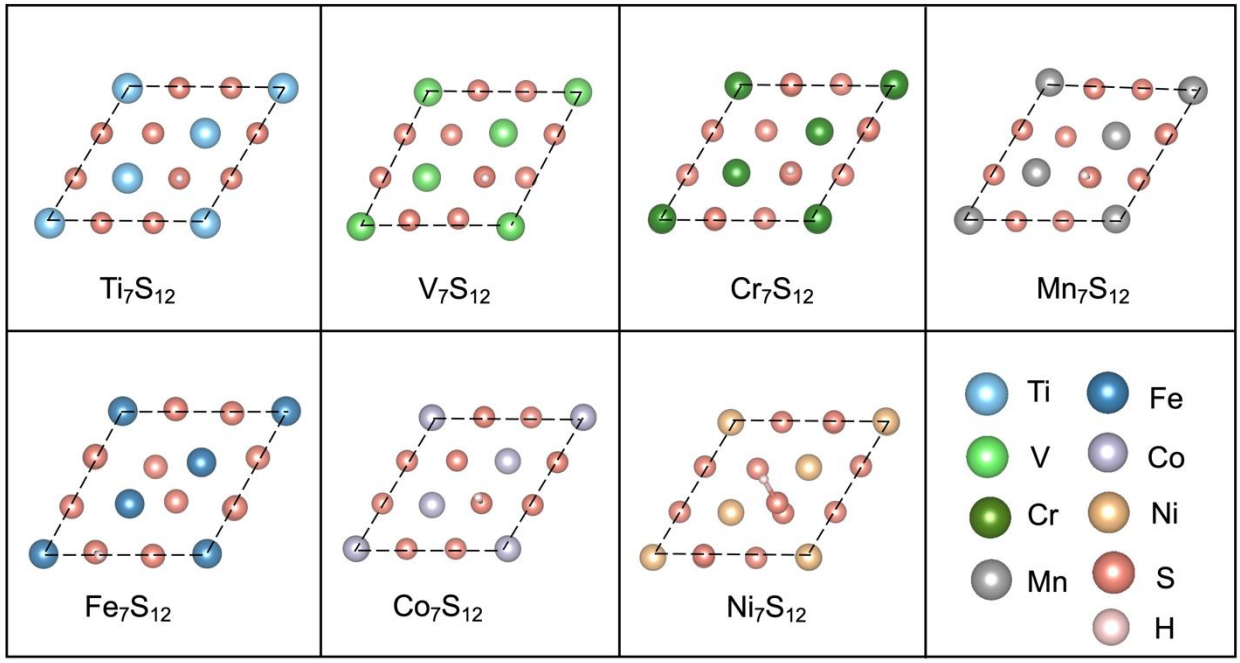

Supplementary Figure 11. Optimized structure for H on ic-2Ds at 8.3% coverage.

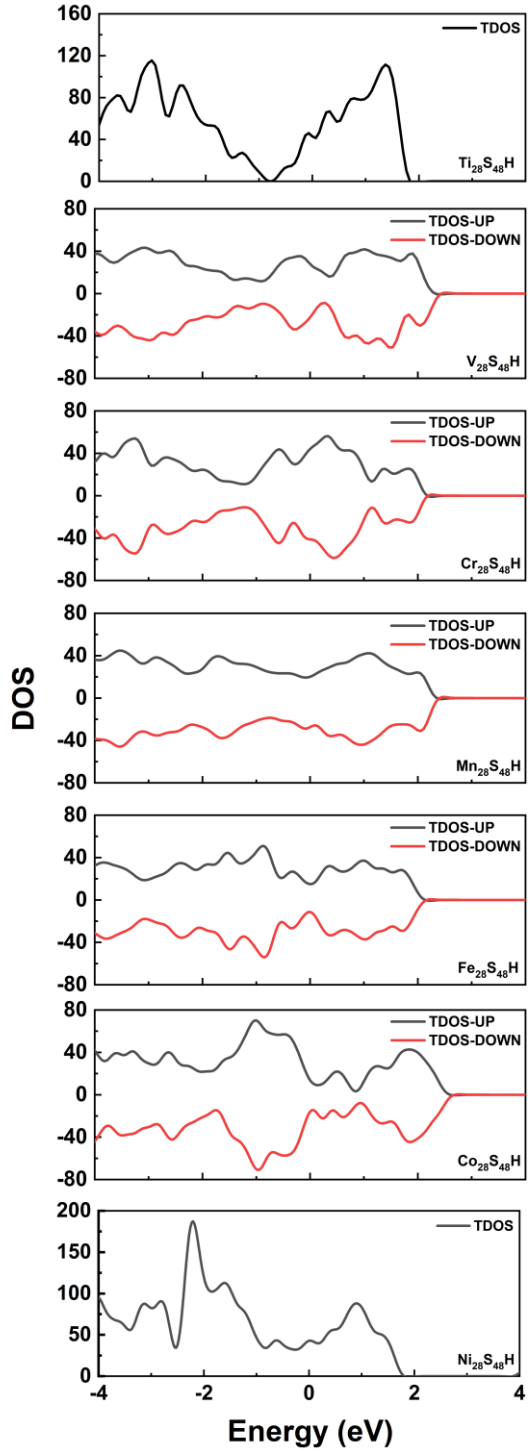

Supplementary Figure 12. Density of states (DOS) after H adsorption on ic-2Ds.

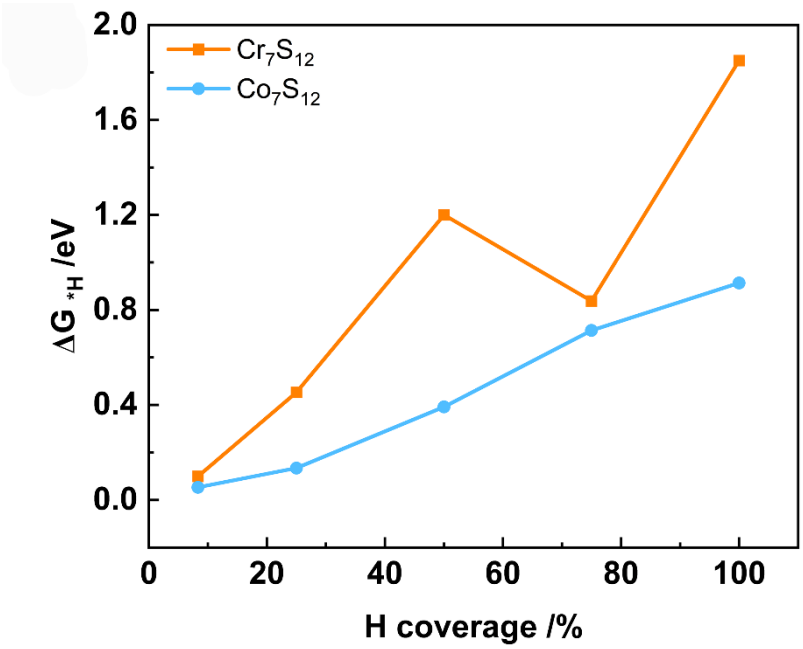

Supplementary Figure 13. HER performance evaluated by ΔG_{*H} under various H coverages.